

ρ^0 Production and Possible Modification in Au+Au and $p + p$ Collisions at $\sqrt{s_{NN}} = 200$ GeV

J. Adams,³ C. Adler,¹³ M.M. Aggarwal,²⁷ Z. Ahammed,⁴⁰ J. Amonett,¹⁹ B.D. Anderson,¹⁹ D. Arkhipkin,¹² G.S. Averichev,¹¹ S.K. Badyal,¹⁸ J. Balewski,¹⁵ O. Barannikova,^{30,11} L.S. Barnby,³ J. Baudot,¹⁷ S. Bekele,²⁶ V.V. Belaga,¹¹ R. Bellwied,⁴³ J. Berger,¹³ B.I. Bezverkhny,⁴⁵ S. Bhardwaj,³¹ A.K. Bhati,²⁷ H. Bichsel,⁴² A. Billmeier,⁴³ L.C. Bland,² C.O. Blyth,³ B.E. Bonner,³² M. Botje,²⁵ A. Boucham,³⁶ A. Brandin,²³ A. Bravar,² R.V. Cadman,¹ X.Z. Cai,³⁵ H. Caines,⁴⁵ M. Calderón de la Barca Sánchez,² J. Carroll,²⁰ J. Castillo,²⁰ D. Cebra,⁵ P. Chaloupka,¹⁰ S. Chattopadhyay,⁴⁰ H.F. Chen,³⁴ Y. Chen,⁶ S.P. Chernenko,¹¹ M. Cherney,⁹ A. Chikanian,⁴⁵ W. Christie,² J.P. Coffin,¹⁷ T.M. Cormier,⁴³ J.G. Cramer,⁴² H.J. Crawford,⁴ D. Das,⁴⁰ S. Das,⁴⁰ A.A. Derevschikov,²⁹ L. Didenko,² T. Dietel,¹³ W.J. Dong,⁶ X. Dong,^{34,20} J.E. Draper,⁵ F. Du,⁴⁵ A.K. Dubey,¹⁶ V.B. Dunin,¹¹ J.C. Dunlop,² M.R. Dutta Majumdar,⁴⁰ V. Eckardt,²¹ L.G. Efimov,¹¹ V. Emelianov,²³ J. Engelage,⁴ G. Eppley,³² B. Erazmus,³⁶ M. Estienne,³⁶ P. Fachini,² V. Faine,² J. Faivre,¹⁷ R. Fatemi,¹⁵ K. Filimonov,²⁰ P. Filip,¹⁰ E. Finch,⁴⁵ Y. Fisyak,² D. Flierl,¹³ K.J. Foley,² J. Fu,⁴⁴ C.A. Gagliardi,³⁷ N. Gagunashvili,¹¹ J. Gans,⁴⁵ M.S. Ganti,⁴⁰ L. Gaudichet,³⁶ F. Geurts,³² V. Ghazikhanian,⁶ P. Ghosh,⁴⁰ J.E. Gonzalez,⁶ O. Grachov,⁴³ O. Grebenyuk,²⁵ S. Gronstal,⁹ D. Grosnick,³⁹ S.M. Guertin,⁶ A. Gupta,¹⁸ T.D. Gutierrez,⁵ T.J. Hallman,² A. Hamed,⁴³ D. Hardtke,²⁰ J.W. Harris,⁴⁵ M. Heinz,⁴⁵ T.W. Henry,³⁷ S. Heppelmann,²⁸ B. Hippolyte,⁴⁵ A. Hirsch,³⁰ E. Hjort,²⁰ G.W. Hoffmann,³⁸ M. Horsley,⁴⁵ H.Z. Huang,⁶ S.L. Huang,³⁴ E. Hughes,⁷ T.J. Humanic,²⁶ G. Igo,⁶ A. Ishihara,³⁸ P. Jacobs,²⁰ W.W. Jacobs,¹⁵ M. Janik,⁴¹ H. Jiang,^{6,20} I. Johnson,²⁰ P.G. Jones,³ E.G. Judd,⁴ S. Kabana,⁴⁵ M. Kaplan,⁸ D. Keane,¹⁹ V.Yu. Khodyrev,²⁹ J. Kiryluk,⁶ A. Kisiel,⁴¹ J. Klay,²⁰ S.R. Klein,²⁰ A. Klyachko,¹⁵ D.D. Koetke,³⁹ T. Kollegger,¹³ M. Kopytine,¹⁹ L. Kotchenda,²³ A.D. Kovalenko,¹¹ M. Kramer,²⁴ P. Kravtsov,²³ V.I. Kravtsov,²⁹ K. Krueger,¹ C. Kuhn,¹⁷ A.I. Kulikov,¹¹ A. Kumar,²⁷ G.J. Kunde,⁴⁵ C.L. Kunz,⁸ R.Kh. Kutuev,¹² A.A. Kuznetsov,¹¹ M.A.C. Lamont,³ J.M. Landgraf,² S. Lange,¹³ B. Lasiuk,⁴⁵ F. Laue,² J. Lauret,² A. Lebedev,² R. Lednický,¹¹ M.J. LeVine,² C. Li,³⁴ Q. Li,⁴³ S.J. Lindenbaum,²⁴ M.A. Lisa,²⁶ F. Liu,⁴⁴ L. Liu,⁴⁴ Z. Liu,⁴⁴ Q.J. Liu,⁴² T. Ljubicic,² W.J. Llope,³² H. Long,⁶ R.S. Longacre,² M. Lopez-Noriega,²⁶ W.A. Love,² T. Ludlam,² D. Lynn,² J. Ma,⁶ Y.G. Ma,³⁵ D. Magestro,²⁶ S. Mahajan,¹⁸ L.K. Mangotra,¹⁸ D.P. Mahapatra,¹⁶ R. Majka,⁴⁵ R. Manweiler,³⁹ S. Margetis,¹⁹ C. Markert,⁴⁵ L. Martin,³⁶ J. Marx,²⁰ H.S. Matis,²⁰ Yu.A. Matulenko,²⁹ C.J. McClain,¹ T.S. McShane,⁹ F. Meissner,²⁰ Yu. Melnick,²⁹ A. Meschanin,²⁹ M.L. Miller,⁴⁵ Z. Milosevich,⁸ N.G. Minaev,²⁹ C. Mironov,¹⁹ A. Mischke,²⁵ D. Mishra,¹⁶ J. Mitchell,³² B. Mohanty,⁴⁰ L. Molnar,³⁰ C.F. Moore,³⁸ M.J. Mora-Corral,²¹ D.A. Morozov,²⁹ V. Morozov,²⁰ M.M. de Moura,³³ M.G. Munhoz,³³ B.K. Nandi,⁴⁰ S.K. Nayak,¹⁸ T.K. Nayak,⁴⁰ J.M. Nelson,³ P.K. Netrakanti,⁴⁰ V.A. Nikitin,¹² L.V. Nogach,²⁹ B. Norman,¹⁹ S.B. Nurushev,²⁹ G. Odyniec,²⁰ A. Ogawa,² V. Okorokov,²³ M. Oldenburg,²⁰ D. Olson,²⁰ G. Paic,²⁶ S.K. Pal,⁴⁰ Y. Panebratsev,¹¹ S.Y. Panitkin,² A.I. Pavlinov,⁴³ T. Pawlak,⁴¹ T. Peitzmann,²⁵ V. Perevoztchikov,² C. Perkins,⁴ W. Peryt,⁴¹ V.A. Petrov,¹² S.C. Phatak,¹⁶ R. Picha,⁵ M. Planinic,⁴⁶ J. Pluta,⁴¹ N. Porile,³⁰ J. Porter,² A.M. Poskanzer,²⁰ M. Potekhin,² E. Potrebenikova,¹¹ B.V.K.S. Potukuchi,¹⁸ D. Prindle,⁴² C. Pruneau,⁴³ J. Putschke,²¹ G. Rai,²⁰ G. Rakness,¹⁵ R. Raniwala,³¹ S. Raniwala,³¹ O. Ravel,³⁶ R.L. Ray,³⁸ S.V. Razin,^{11,15} D. Reichhold,³⁰ J.G. Reid,⁴² G. Renault,³⁶ F. Retiere,²⁰ A. Ridiger,²³ H.G. Ritter,²⁰ J.B. Roberts,³² O.V. Rogachevski,¹¹ J.L. Romero,⁵ A. Rose,⁴³ C. Roy,³⁶ L.J. Ruan,^{34,2} R. Sahoo,¹⁶ I. Sakrejda,²⁰ S. Salur,⁴⁵ J. Sandweiss,⁴⁵ I. Savin,¹² J. Schambach,³⁸ R.P. Scharenberg,³⁰ N. Schmitz,²¹ L.S. Schroeder,²⁰ K. Schweda,²⁰ J. Seger,⁹ P. Seyboth,²¹ E. Shahaliev,¹¹ M. Shao,³⁴ W. Shao,⁷ M. Sharma,²⁷ K.E. Shestermanov,²⁹ S.S. Shimanskii,¹¹ R.N. Singaraju,⁴⁰ F. Simon,²¹ G. Skoro,¹¹ N. Smirnov,⁴⁵ R. Snellings,²⁵ G. Sood,²⁷ P. Sorensen,²⁰ J. Sowinski,¹⁵ J. Speltz,¹⁷ H.M. Spinka,¹ B. Srivastava,³⁰ T.D.S. Stanislaus,³⁹ R. Stock,¹³ A. Stolpovsky,⁴³ M. Strikhanov,²³ B. Stringfellow,³⁰ C. Struck,¹³ A.A.P. Suaide,³³ E. Sugarbaker,²⁶ C. Suire,² M. Šumbera,¹⁰ B. Surrow,² T.J.M. Symons,²⁰ A. Szanto de Toledo,³³ P. Szarwas,⁴¹ A. Tai,⁶ J. Takahashi,³³ A.H. Tang,^{2,25} D. Thein,⁶ J.H. Thomas,²⁰ S. Timoshenko,²³ M. Tokarev,¹¹ M.B. Tonjes,²² T.A. Trainor,⁴² S. Trentalange,⁶ R.E. Tribble,³⁷ O. Tsai,⁶ T. Ullrich,² D.G. Underwood,¹ G. Van Buren,² A.M. VanderMolen,²² R. Varma,¹⁴ I. Vasilevski,¹² A.N. Vasiliev,²⁹ R. Vernet,¹⁷ S.E. Vigdor,¹⁵ Y.P. Viyogi,⁴⁰ S.A. Voloshin,⁴³ M. Vznuzdaev,²³ W. Wagoner,⁹ F. Wang,³⁰ G. Wang,⁷ G. Wang,¹⁹ X.L. Wang,³⁴ Y. Wang,³⁸ Z.M. Wang,³⁴ H. Ward,³⁸ J.W. Watson,¹⁹ J.C. Webb,¹⁵ R. Wells,²⁶ G.D. Westfall,²² C. Whitten Jr.,⁶ H. Wieman,²⁰ R. Willson,²⁶ S.W. Wissink,¹⁵ R. Witt,⁴⁵ J. Wood,⁶ J. Wu,³⁴ N. Xu,²⁰ Z. Xu,² Z.Z. Xu,³⁴ E. Yamamoto,²⁰ P. Yepes,³² V.I. Yurevich,¹¹ B. Yuting,²⁵ Y.V. Zanevski,¹¹ H. Zhang,^{45,2} W.M. Zhang,¹⁹ Z.P. Zhang,³⁴ Z.P. Zhaomin,³⁴ Z.P. Zizong,³⁴ P.A. Żołnierczuk,¹⁵ R. Zoukarneev,¹² J. Zoukarneeva,¹² and A.N. Zubarev¹¹

¹Argonne National Laboratory, Argonne, Illinois 60439

- ²Brookhaven National Laboratory, Upton, New York 11973
³University of Birmingham, Birmingham, United Kingdom
⁴University of California, Berkeley, California 94720
⁵University of California, Davis, California 95616
⁶University of California, Los Angeles, California 90095
⁷California Institute of Technology, Pasadena, California 91125
⁸Carnegie Mellon University, Pittsburgh, Pennsylvania 15213
⁹Creighton University, Omaha, Nebraska 68178
¹⁰Nuclear Physics Institute AS CR, Řež/Prague, Czech Republic
¹¹Laboratory for High Energy (JINR), Dubna, Russia
¹²Particle Physics Laboratory (JINR), Dubna, Russia
¹³University of Frankfurt, Frankfurt, Germany
¹⁴Indian Institute of Technology, Mumbai, India
¹⁵Indiana University, Bloomington, Indiana 47408
¹⁶Institute of Physics, Bhubaneswar 751005, India
¹⁷Institut de Recherches Subatomiques, Strasbourg, France
¹⁸University of Jammu, Jammu 180001, India
¹⁹Kent State University, Kent, Ohio 44242
²⁰Lawrence Berkeley National Laboratory, Berkeley, California 94720
²¹Max-Planck-Institut für Physik, Munich, Germany
²²Michigan State University, East Lansing, Michigan 48824
²³Moscow Engineering Physics Institute, Moscow Russia
²⁴City College of New York, New York City, New York 10031
²⁵NIKHEF, Amsterdam, The Netherlands
²⁶Ohio State University, Columbus, Ohio 43210
²⁷Panjab University, Chandigarh 160014, India
²⁸Pennsylvania State University, University Park, Pennsylvania 16802
²⁹Institute of High Energy Physics, Protvino, Russia
³⁰Purdue University, West Lafayette, Indiana 47907
³¹University of Rajasthan, Jaipur 302004, India
³²Rice University, Houston, Texas 77251
³³Universidade de Sao Paulo, Sao Paulo, Brazil
³⁴University of Science & Technology of China, Anhui 230027, China
³⁵Shanghai Institute of Nuclear Research, Shanghai 201800, P.R. China
³⁶SUBATECH, Nantes, France
³⁷Texas A&M University, College Station, Texas 77843
³⁸University of Texas, Austin, Texas 78712
³⁹Valparaiso University, Valparaiso, Indiana 46383
⁴⁰Variable Energy Cyclotron Centre, Kolkata 700064, India
⁴¹Warsaw University of Technology, Warsaw, Poland
⁴²University of Washington, Seattle, Washington 98195
⁴³Wayne State University, Detroit, Michigan 48201
⁴⁴Institute of Particle Physics, CCNU (HZNU), Wuhan, 430079 China
⁴⁵Yale University, New Haven, Connecticut 06520
⁴⁶University of Zagreb, Zagreb, HR-10002, Croatia

(Dated: October 15, 2018)

We report results on $\rho(770)^0 \rightarrow \pi^+\pi^-$ production at midrapidity in $p+p$ and peripheral Au+Au collisions at $\sqrt{s_{NN}} = 200$ GeV. This is the first direct measurement of $\rho(770)^0 \rightarrow \pi^+\pi^-$ in heavy-ion collisions. The measured ρ^0 peak in the invariant mass distribution is shifted by ~ 40 MeV/ c^2 in minimum bias $p+p$ interactions and ~ 70 MeV/ c^2 in peripheral Au+Au collisions. The ρ^0 mass shift is dependent on transverse momentum and multiplicity. The modification of the ρ^0 meson mass, width, and shape due to phase space and dynamical effects are discussed.

PACS numbers: 25.75.Dw, 13.85.Hd

In-medium modification of the ρ meson due to the effects of increasing temperature and density has been proposed as a possible signal of a phase transition of nuclear matter to a deconfined plasma of quarks and gluons, which is expected to be accompanied by the restoration of chiral symmetry [1].

The ρ^0 meson measured in the dilepton channel probes all stages of the system formed in relativistic heavy-ion collisions because the dileptons have negligible final state interactions with the hadronic environment. Heavy-ion experiments at CERN indicate an enhanced dilepton production cross section in the invariant mass range of 200-

600 MeV/c² [2]. The study of the dilepton decay channel currently relies on model calculations based on a so-called “hadronic cocktail”, a superposition of the expected contributions to the dilepton spectrum [1, 2, 3]. The present hadronic decay measurement, $\rho(770)^0 \rightarrow \pi^+\pi^-$, is the first of its kind in heavy-ion collisions and provides experimental data to help constrain the input to the hadronic cocktail used for such studies.

Even in the absence of the phase transition, at normal nuclear density, temperature and density dependent modifications of the ρ^0 meson are expected to be measurable. Effects such as phase space [4, 5, 6, 7, 8, 9, 10, 11, 12] and dynamical interactions with matter [6, 8, 10] may modify the ρ^0 mass, width, and shape. These modifications of the ρ^0 properties take place close to kinetic freeze-out (vanishing elastic collisions), in a dilute hadronic gas at late stages of heavy-ion collisions. At such low matter density, the proposed modifications are expected to be small, but observable. The effects of phase space due to the rescattering of pions, $\pi^+\pi^- \rightarrow \rho^0 \rightarrow \pi^+\pi^-$, and Bose-Einstein correlations between pions from ρ^0 decay and pions in the surrounding matter are present in $p+p$ [5, 6, 8, 12] and Au+Au [4, 6, 7, 8, 9, 10, 11] collisions. The interference between different pion scattering channels can effectively distort the line shape of resonances [13]. Dynamical effects due to the ρ^0 interacting with the surrounding matter are also expected to be present in $p+p$ and Au+Au interactions, and have been evaluated for the latter [6, 8, 10].

Since the ρ^0 lifetime of $c\tau = 1.3$ fm is small with respect to the lifetime of the system formed in Au+Au collisions, the ρ^0 meson is expected to decay, regenerate, and rescatter all the way through kinetic freeze-out. In the context of statistical models, the measured ρ^0 yield should reflect conditions at kinetic freeze-out rather than at chemical freeze-out (vanishing inelastic collisions) [6, 8, 9, 11, 14]. In $p+p$ collisions, the ρ^0 meson is expected to be produced predominantly by string fragmentation. The measurement of the ρ^0 meson in $p+p$ and Au+Au interactions at the same nucleon-nucleon c.m. system energy can provide insight for understanding the dynamics of these systems.

The detector system used for these studies was the Solenoidal Tracker at RHIC (STAR). The main tracking device within STAR is the time projection chamber (TPC) [15] located inside a 0.5 T solenoidal magnetic field. In addition to providing momentum information, the TPC provides particle identification for charged particles by measuring their ionization energy loss (dE/dx). In Au+Au collisions, a minimum bias trigger was defined using coincidences between two zero degree calorimeters that measured the spectator neutrons. In $p+p$ collisions, the minimum bias trigger was defined using coincidences between two beam-beam counters that measured the charged particle multiplicity in forward pseudorapidities ($3.3 < |\eta| < 5.0$). This trigger is sensitive to nonsingly diffractive (NSD) events, with negligible bias on yields [16]. Approximately 11×10^6 minimum bias $p+p$ events,

1.5×10^6 high multiplicity $p+p$ events, and 1.2×10^6 events in the peripheral centrality class corresponding to 40-80% of the inelastic hadronic Au+Au cross section were used for this analysis. The beam energy was $\sqrt{s_{NN}} = 200$ GeV. High multiplicity $p+p$ events were those from the top 10% of the minimum bias $p+p$ multiplicity distribution for $|\eta| < 0.5$. Since the pion daughters from ρ^0 decays originate at the interaction point, only tracks whose distance of closest approach to the primary interaction vertex was less than 3 cm were selected. Charged pions were selected by requiring their dE/dx to be within 3 standard deviations (3σ) of the expected mean. In order to enhance track quality [17], candidate decay daughters were also required to have $|\eta| < 0.8$ and transverse momenta $p_T > 0.2$ GeV/c.

The main focus of this study was the decay channel $\rho^0 \rightarrow \pi^+\pi^-$, which has a branching ratio of $\sim 100\%$. Similar to previous e^+e^- and $p+p$ measurements, the ρ^0 sample studied did not select exclusively on the $\ell=1$ $\pi^+\pi^-$ channel [18, 19, 20, 21, 22, 23, 24, 25, 26]. The measurement was performed calculating the invariant mass for each $\pi^+\pi^-$ pair in an event. The resulting invariant mass distribution was then compared to a reference distribution calculated from the geometric mean of the invariant mass distributions obtained from uncorrelated $\pi^+\pi^+$ and $\pi^-\pi^-$ pairs from the same events. The $\pi^+\pi^-$ invariant mass distribution ($M_{\pi\pi}$) and the like-sign reference distribution were normalized to each other at $M_{\pi\pi} \gtrsim 1.5$ GeV/c². The resulting raw distributions for minimum bias $p+p$ and peripheral Au+Au collisions at midrapidity ($|y| < 0.5$) for a particular p_T bin are shown in Fig. 1. The signal to background is 1/10 in minimum bias $p+p$ and 1/200 in peripheral Au+Au collisions. The p_T coverage of the $\pi^+\pi^-$ pair is $0.2 \leq p_T \leq 2.8$ GeV/c for minimum bias $p+p$ and $0.2 \leq p_T \leq 2.2$ GeV/c for peripheral Au+Au collisions.

The solid black line in Fig. 1 is the sum of all the contributions in the hadronic cocktail. The K_S^0 was fit to a Gaussian (dotted line). The ω (light grey line) and $K^*(892)^0$ (dash-dotted line) shapes were obtained from the HIJING event generator [27], with the kaon being misidentified as a pion in the case of the K^{*0} . The $\rho^0(770)$ (dashed line), the $f_0(980)$ (dotted line) and the $f_2(1270)$ (dark grey line) were fit by relativistic Breit-Wigner functions [28] $BW = M_{\pi\pi}M_0\Gamma/[(M_0^2 - M_{\pi\pi}^2)^2 + M_0^2\Gamma^2]$ times the Boltzmann factor [5, 6, 7, 8] $PS = (M_{\pi\pi}/\sqrt{M_{\pi\pi}^2 + p_T^2}) \times \exp(-\sqrt{M_{\pi\pi}^2 + p_T^2}/T)$ to account for phase space. Here, T is the temperature at which the resonance is emitted [6] and $\Gamma = \Gamma_0 \times (M_0/M_{\pi\pi}) \times [(M_{\pi\pi}^2 - 4m_\pi^2)/(M_0^2 - 4m_\pi^2)]^{(2\ell+1)/2}$ is the momentum dependent width [28]. The masses of K_S^0 , ρ^0 , f_0 , and f_2 were free parameters in the fit, and the widths of ρ^0 , f_0 and f_2 were fixed according to [29]. The uncorrected yields of K_S^0 , ρ^0 , ω , f_0 , and f_2 were free parameters in the fit while the K^{*0} fraction was fixed according to the $K^{*0} \rightarrow \pi K$ measurement. The ρ^0 , ω , K^{*0} , f_0 , and f_2 distributions were corrected for the detector acceptance and efficiency determined from a detailed simulation of the TPC re-

sponse using GEANT [17]. For the particular p_T bin depicted in Fig. 1 and the invariant mass region shown, this correction is approximately constant and is $\sim 25\%$ for minimum bias $p + p$ and varies from $\sim 25\%$ to $\sim 35\%$ for peripheral Au+Au collisions. The number of degrees of freedom (d.o.f.) from the fits was 196 and the typical $\chi^2/\text{d.o.f.}$ was 1.4. In the minimum bias $p + p$ invariant mass distribution shown in Fig. 1, $\pi^\pm\pi^\pm$ Bose-Einstein correlations have been taken into account. These affect the distribution for $M_{\pi\pi} < 0.45 \text{ GeV}/c^2$.

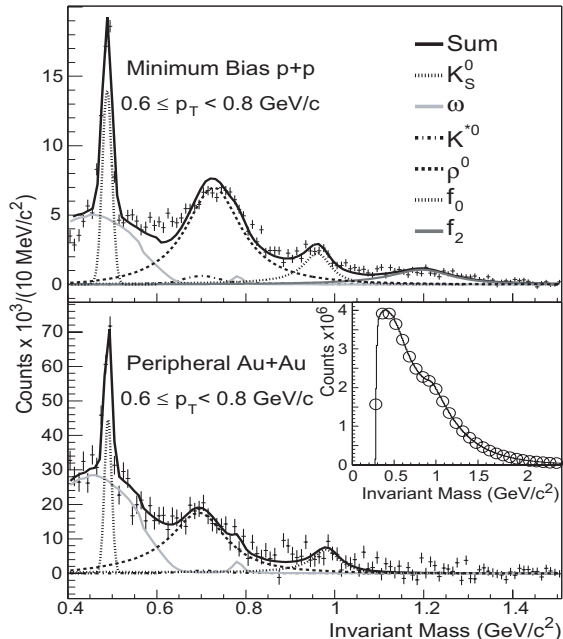


FIG. 1: The raw $\pi^+\pi^-$ invariant mass distributions after subtraction of the like-sign reference distribution for minimum bias $p + p$ (top) and peripheral Au+Au (bottom) interactions. The inset plot corresponds to the raw $\pi^+\pi^-$ invariant mass distribution (solid line) and the like-sign reference distributions (open circles) for peripheral Au+Au collisions.

The ρ^0 mass is shown as a function of p_T in Fig. 2 for peripheral Au+Au, high multiplicity $p + p$, and minimum bias $p + p$ interactions. The ρ^0 mass was obtained by fitting the data to a relativistic p -wave ($\ell = 1$) Breit-Wigner function times a factor which accounts for phase space (BW \times PS) in the hadronic cocktail. Since the phase space factor modifies the position of the peak for the BW function, the mass derived from the BW \times PS fit may be shifted compared to the peak of the experimental invariant mass distribution and to the peak of the BW function alone. The ρ^0 peak was also fit to a relativistic p -wave BW function excluding the PS factor in the hadronic cocktail; however, the fit failed to reproduce the ρ^0 line shape, and underestimated the position of the peak in general, particularly at low p_T . This measurement does not have sufficient sensitivity to permit a systematic study of the ρ^0 width. Therefore, for the cocktail fits in this analysis, the ρ^0 width was fixed at $\Gamma_0 = 160 \text{ MeV}/c^2$, consistent with folding the ρ^0 natural

width ($150.9 \pm 2.0 \text{ MeV}/c^2$ [29]) with the intrinsic resolution of the detector [17]. In Au+Au collisions, the temperature used in the PS factor was $T = 120 \text{ MeV}$ [6], while in $p + p$, $T = 160 \text{ MeV}$ [30].

The ρ^0 mass at $|y| < 0.5$ for minimum bias $p + p$, high multiplicity $p + p$, and peripheral Au+Au collisions at $\sqrt{s} = 200 \text{ GeV}$ seems to increase as a function of p_T and is systematically lower than the value reported by [23]. The ρ^0 mass measured in peripheral Au+Au collisions is lower than the minimum bias $p + p$ measurement. The ρ^0 mass for high multiplicity $p + p$ interactions is lower than for minimum bias $p + p$ interactions for all p_T bins, showing that the ρ^0 mass is also multiplicity dependent. Recent calculations are not able to reproduce the ρ^0 mass measured in peripheral Au+Au collisions without introducing in-medium modification of the ρ^0 meson [6, 7, 8, 9, 10, 11].

Previous observations of the ρ meson in e^+e^- [31, 32, 33] and $p + p$ interactions [23] indicate that the ρ^0 line shape is considerably distorted from a p -wave BW function. A mass shift of $-30 \text{ MeV}/c^2$ or larger was observed in e^+e^- collisions at $\sqrt{s} = 90 \text{ GeV}$ [31, 32, 33]. In the $p + p$ measurement at $\sqrt{s} = 27.5 \text{ GeV}$ [23], a ρ^0 mass of $0.7626 \pm 0.0026 \text{ GeV}/c^2$ was obtained from a fit to the BW \times PS function [12, 23]. However, in this measurement the position of the ρ^0 peak is lower than the average of the ρ^0 mass measured in e^+e^- interactions [29] by $\sim 30 \text{ MeV}/c^2$ [23]. This result is the only $p + p$ measurement used in the hadroproduced ρ^0 mass average reported in [29].

In comparison to the in-medium ρ^0 production in hadronic Au+Au interactions, no modifications of the ρ^0 properties are expected for coherent ρ^0 production in ultraperipheral heavy-ion collisions, where (in lowest order) at impact parameters $b > 2R_A$, a photon emitted by one gold ion fluctuates into a virtual ρ^0 meson state, which scatters diffractively from the other nucleus. The ρ^0 line shape in ultra-peripheral collisions measured with the STAR detector [28] is reproduced by a BW plus Söding interference term, with the ρ^0 mass and width consistent with their natural values reported in [29].

One uncertainty in the hadronic cocktail fit depicted in Fig. 1 is the possible existence of correlations of unknown origin near the ρ^0 mass. An example is correlations in the invariant mass distribution from particles like the $f_0(600)$ which are not well established [29]. The ω yield in the hadronic cocktail fits may account for some of these contributions and may cause the apparent decrease in the ρ^0/ω ratio between minimum bias $p + p$ and peripheral Au+Au interactions. In order to evaluate the systematic uncertainty in the ρ^0 mass due to poorly known contributions in the hadronic cocktail, the ρ^0 mass was obtained by fitting the peak to the BW \times PS function plus an exponential function representing these contributions. Using this procedure, the ρ^0 mass is systematically higher than the mass obtained from the hadronic cocktail fit. This uncertainty is the main contribution to the systematic uncertainties shown in Fig. 2 and it can be as large as

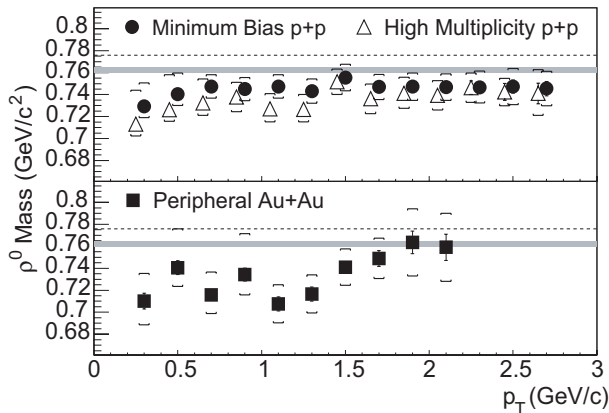


FIG. 2: The ρ^0 mass as a function of p_T for minimum bias $p + p$ (filled circles), high multiplicity $p + p$ (open triangles), and peripheral Au+Au (filled squares) collisions. The error bars indicate the systematic uncertainty. Statistical errors are negligible. The ρ^0 mass was obtained by fitting the data to the BW \times PS functional form described in the text. The dashed lines represent the average of the ρ^0 mass measured in e^+e^- [29]. The shaded areas indicate the ρ^0 mass measured in $p + p$ collisions [23]. The open triangles have been shifted downward on the abscissa by 50 MeV/c for clarity.

~ 35 MeV/ c^2 for low p_T . Other contributions to the systematic errors shown in Fig. 2 result from uncertainty in the measurement of particle momenta of ~ 3 MeV/ c^2 (this leads to a mass resolution of ~ 8 MeV/ c^2 at the ρ^0 mass) and from the hadronic cocktail fits themselves of ~ 13 MeV/ c^2 . The systematic uncertainties are common to all p_T bins and are correlated between the $p + p$ and peripheral Au+Au measurements.

The corrected invariant yields [$d^2N/(2\pi p_T dp_T dy)$] at $|y| < 0.5$ as a function of p_T for peripheral Au+Au and minimum bias $p + p$ interactions are shown in Fig. 3. In $p + p$ interactions, a power-law fit was used to extract the ρ^0 yield per unit of rapidity around midrapidity. The fit yielded $dN/dy = 0.259 \pm 0.002(\text{stat}) \pm 0.039(\text{syst})$ and $\langle p_T \rangle = 0.616 \pm 0.002(\text{stat}) \pm 0.062(\text{syst})$ GeV/c. In Au+Au collisions, an exponential fit in $m_T - m_0$, where $m_0 = 0.769$ MeV/ c^2 is the average ρ^0 mass reported in [29], was used to extract the ρ^0 yield and the inverse slope. The fit yielded $dN/dy = 5.4 \pm 0.1(\text{stat}) \pm 1.2(\text{syst})$ and an inverse slope of $318 \pm 4(\text{stat}) \pm 38(\text{syst})$ MeV [$\langle p_T \rangle = 0.83 \pm 0.01(\text{stat}) \pm 0.10(\text{syst})$ GeV/c]. The main contributions to the systematic uncertainties quoted are due to the tracking efficiency ($\sim 8\%$) and the normalization between the $M_{\pi\pi}$ and the like-sign reference distributions ($\sim 9\%$ for minimum bias $p + p$ and $\sim 19\%$ for peripheral Au+Au collisions).

The ρ^0/π^- ratio is $0.183 \pm 0.001(\text{stat}) \pm 0.027(\text{syst})$ for minimum bias $p + p$, and $0.169 \pm 0.003(\text{stat}) \pm 0.037(\text{syst})$ for peripheral Au+Au collisions. The comparison with measurements in e^+e^- [18, 19, 20], $p + p$ [21, 22, 23, 24], K^+p [25], and π^-p [26] interactions at different c.m. system energies is shown in Fig. 4. The ρ^0/π^- ratios from

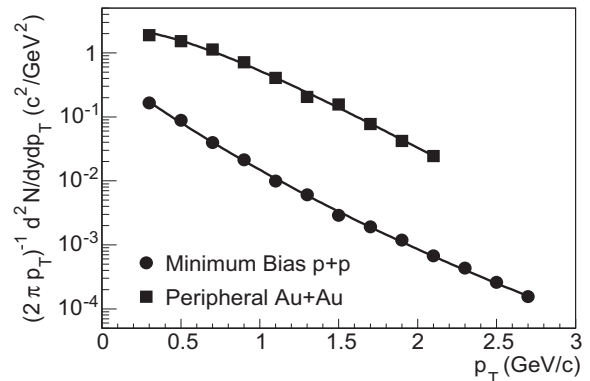


FIG. 3: The p_T distributions at $|y| < 0.5$ for minimum bias $p + p$ and peripheral Au+Au collisions. See text for an explanation of the functions used to fit the data. The errors shown are statistical only and smaller than the symbols.

minimum bias $p + p$ and peripheral Au+Au interactions are comparable.

The ρ^0/π^- ratios from statistical model calculations [8, 9, 14] for Au+Au collisions are considerably lower than the measurement presented in Fig. 4. The larger ρ^0/π^- ratio measured may be due to the interplay between the rescattering of the ρ^0 decay products and ρ^0 regeneration.

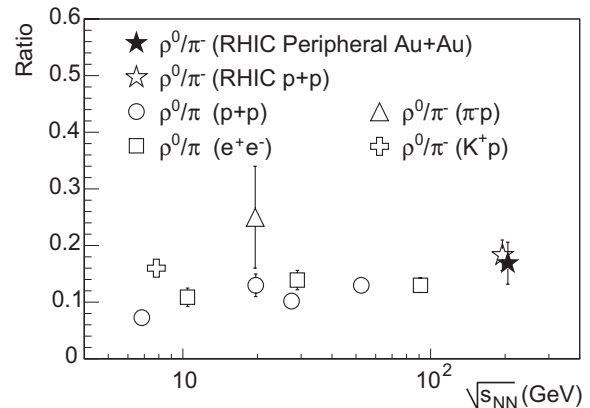


FIG. 4: ρ^0/π^- ratios as a function of c.m. system energy. The ratios are from measurements in e^+e^- collisions at 10.45 GeV [18], 29 GeV [19] and 91 GeV [20] c.m. system energy, $p + p$ at 6.8 GeV [21], 19.7 GeV [22], 27.5 GeV [23], and 52.5 GeV [24], K^+p at 7.82 GeV [25] and π^-p at 19.6 GeV [26]. The errors on the ratios at $\sqrt{s_{NN}} = 200$ GeV are the quadratic sum of the statistical and systematic errors. The ratios at $\sqrt{s_{NN}} = 200$ GeV are offset from one another for clarity.

In conclusion, we have presented results on $\rho(770)^0$ production at midrapidity in minimum bias $p + p$ and peripheral Au+Au collisions at $\sqrt{s_{NN}} = 200$ GeV. This is the first direct measurement of $\rho^0(770) \rightarrow \pi^+\pi^-$ in heavy-ion collisions. The ρ^0 mass seems to increase slightly as a function of p_T , and to decrease with multiplicity. The measured ρ^0 peak in the invariant mass distribution is lower than previous measurements reported in [29] by

~ 40 MeV/ c^2 in minimum bias $p+p$ interactions and ~ 70 MeV/ c^2 in peripheral Au+Au collisions. Similar mass shifts were observed in e^+e^- and $p+p$ interactions. Dynamical interactions with the surrounding matter, interference between various $\pi^+\pi^-$ scattering channels, phase space distortions due to the rescattering of pions forming ρ^0 , and Bose-Einstein correlations between ρ^0 decay daughters and pions in the surrounding matter are possible explanations for the apparent modification of the ρ^0 meson properties. The ρ^0/π^- ratio in peripheral Au+Au collisions is higher than predicted by statistical calculations, and is comparable to the measured value in minimum bias $p+p$ interactions. Further measurements of the ρ^0 meson, along with other resonance particles, can provide important information on the dynamics of relativistic collisions and help in understanding the proper-

ties of nuclear matter under extreme conditions.

We thank M. Bleicher, P. Braun-Munzinger, W. Broniowski, G.E. Brown, W. Florkowski, P. Kolb, G.D. Laferty, S. Pratt, R. Rapp, and E. Shuryak for valuable discussions. We thank the RHIC Operations Group and RCF at BNL, and the NERSC Center at LBNL for their support. This work was supported in part by the HENP Divisions of the Office of Science of the U.S. DOE; the U.S. NSF; the BMBF of Germany; IN2P3, RA, RPL, and EMN of France; EPSRC of the United Kingdom; FAPESP of Brazil; the Russian Ministry of Science and Technology; the Ministry of Education and the NNSFC of China; SFOM of the Czech Republic, FOM and UU of the Netherlands, DAE, DST, and CSIR of the Government of India; the Swiss NSF.

-
- [1] R. Rapp and J. Wambach, *Adv. Nucl. Phys.* **25**, 1 (2000).
 - [2] G. Agakishiev *et al.*, *Phys. Rev. Lett.* **75**, 1272 (1995); B. Lenkeit *et al.*, *Nucl. Phys. A* **661**, 23 (1999).
 - [3] P. Huonvinen *et al.*, *Phys. Rev. C* **66**, 014903 (2002).
 - [4] H.W. Barz *et al.*, *Phys. Lett. B* **265**, 219 (1991).
 - [5] P. Braun-Munzinger (private communication).
 - [6] E.V. Shuryak and G.E. Brown, *Nucl. Phys. A* **717**, 322 (2003).
 - [7] P.F. Kolb and M. Prakash, *nucl-th/0301007*.
 - [8] R. Rapp, *hep-ph/0305011*.
 - [9] W. Broniowski *et al.*, *nucl-th/0306034*.
 - [10] M. Bleicher and H. Stöcker, *J. Phys. G* **30**, S111 (2004).
 - [11] S. Pratt and W. Bauer, *nucl-th/0308087*.
 - [12] P. Granet *et al.*, *Nucl. Phys. B* **140**, 389 (1978).
 - [13] R.S. Longacre, *nucl-th/0303068*.
 - [14] P. Braun-Munzinger *et al.*, *Phys. Lett. B* **518**, 41 (2001); J. Stachel (private communication).
 - [15] M. Anderson *et al.*, *Nucl. Instrum. Meth. A* **499**, 659 (2003).
 - [16] C. Adams *et al.*, *nucl-ex/0305015*.
 - [17] C. Adler *et al.*, *Phys. Rev. Lett.* **87**, 112303 (2001).
 - [18] H. Albrecht *et al.*, *Z. Phys. C* **61**, 1 (1994).
 - [19] M. Derrick *et al.*, *Phys. Lett. B* **158**, 519 (1985).
 - [20] Y. J. Pei *et al.*, *Z. Phys. C* **72**, 39 (1996).
 - [21] V. Blobel *et al.*, *Phys. Lett. B* **48**, 73 (1974).
 - [22] R. Singer *et al.*, *Phys. Lett. B* **60**, 385 (1976).
 - [23] M. Aguilar-Benitez *et al.*, *Z. Phys. C* **50**, 405 (1991).
 - [24] D. Drijard *et al.*, *Z. Phys. C* **9**, 293 (1981).
 - [25] P.V. Chliapnikov *et al.*, *Nucl. Phys. B* **176**, 303 (1980).
 - [26] F.C. Winkelmann *et al.*, *Phys. Lett. B* **56**, 101 (1975).
 - [27] X.N. Wang and M. Gyulassy, *Phys. Rev. D* **44**, 3501 (1991); *Compt. Phys. Commun.* **83**, 307 (1994).
 - [28] C. Adler *et al.*, *Phys. Rev. Lett.* **89**, 272302 (2002).
 - [29] K. Hagiwara *et al.*, *Phys. Rev. D* **66**, 010001 (2002).
 - [30] F. Becattini, *Nucl. Phys. A* **702**, 336 (2002).
 - [31] P.D. Acton *et al.*, *Z. Phys. C* **56**, 521 (1992); G.D. Laferty, *Z. Phys. C* **60**, 659 (1993).
 - [32] K. Ackerstaff *et al.*, *Eur. Phys. J. C* **5**, 411 (1998).
 - [33] D. Buskulic *et al.*, *Z. Phys. C* **69**, 379 (1996).